Eur. Phys. J. B **25**, 307–311 (2002)
DOI: 10.1140/epjb/e20020035

THE EUROPEAN PHYSICAL JOURNAL B
EDP Sciences

Some experimental and theoretical studies on the Mn magnetic moment in $Y(Ni_{1-x}Mn_x)_2B_2C$

F.S. da Rocha[1], G.L.F. Fraga[1], D.E. Brandão[1], C.M. Granada[2], C.M. da Silva[2,a], and A.A. Gomes[3]

[1] Instituto de Física – UFRGS, Porto Alegre, Brazil
[2] Departamento de Física – UFSM, Santa Maria, Brazil
[3] Centro Brasileiro de Pesquisas Físicas/CNPq, Rua Xavier Sigaud 150, Rio de Janeiro 22290-180, Brazil

Received 23 April 2001 and Received in final form 29 October 2001

Abstract. The magnetic moment of the Mn impurities was obtained from magnetization measurements of $Y(Ni_{1-x}Mn_x)_2B_2C$ as a function of the concentration x less than 0.15. Using the coherent potential approximation and starting from $3d$ density of states, obtained from the first principles calculations, the magnetic moments are obtained within a two sublattice model. For adequately estimated values of the Coulomb interactions U, the position of the energy level of Mn and adopting values for the intersublattice hybridization term, a qualitative agreement with the observed experimental data is obtained.

PACS. 74.25.Jb Electronic structure – 75.10.Lp Band and itinerant models – 75.30.Hx Magnetic impurity interactions – 74.25.Ha Magnetic properties

1 Introduction

Recently a new kind of borocarbide quaternary intermetallic compound, following the RM_2B_2C stoichiometric formula, has been discovered [1]. In this formula R is a rare-earth, Y or Sc atoms and M is a transition element like Ni, Co or Pd. The crystal structure of these materials is a body centered tetragonal, space group I4/mmm, with RC planes alternating with M_2B_2 layers. This structure is highly anisotropic with c/a approximately equal to three.

Some remarks are worthwhile about the origin of superconductivity in these compounds. Contrary to high T_c materials, a phononic mechanism is usually invoked for the origin of the superconducting pairs. The origin of the quite strong electron-phonon coupling has been recently discussed [2]. Electronic band calculations of borocarbides show a clear three dimensional nature of these compounds [3,4], since the contribution of both the xy plane and z direction to the band widths are of the same order of magnitude.

Another specificity of these materials, similarly to Laves phases and Heusler compounds, is the possibility of selective solution of impurities in the M_2B_2 layer, replacing M atoms by other transition metals. Examples of this are given by alloying effects observed in $Y(Ni_{1-x}M_x)_2B_2C$, with M = Co, (Co, Cu), (Ru, Fe, Co) [5–7]. Interestingly enough, it is experimentally observed that Fe and Co impurities *do not* form a magnetic moment in these materials.

The main motivation of the present study is to investigate the electronic structure and the possible magnetic moment formation on Mn impurity atoms in $Y(Ni_{1-x}Mn_x)_2B_2C$ pseudoquaternary compounds, for which experimental data for the saturation magnetization have been obtained. The presence of impurities, selectively replacing Ni atoms may show a possible concentration x dependence of the Mn magnetic moment $m(x)$. Note that for $x = 0$ no magnetic moment is refereed to exist in this compound.

The model to be used in the description of these transition metal magnetic moments requires the calculation of the electronic structure of the conduction electrons of the pure compound. If selective disorder is present, it should be described within the coherent potential approximation (CPA) [8], since a strong impurity perturbation is associated with the charge difference ΔZ between Ni and Mn. Since the Ni $- 3d$ local density of states of the pure compound has been calculated from first principles methods, it is possible to analyze the effect of intersublattice hopping from the value of the so obtained magnetic moment.

The purpose of this calculation is to show the role of the impurity energy level ε_{Mn}, the Coulomb d-interactions U_{Mn} and the intersublattice hopping contribution to the Mn magnetic moment formation and in particular its concentration dependence.

[a] e-mail: dasilva@ccne.ufsm.br

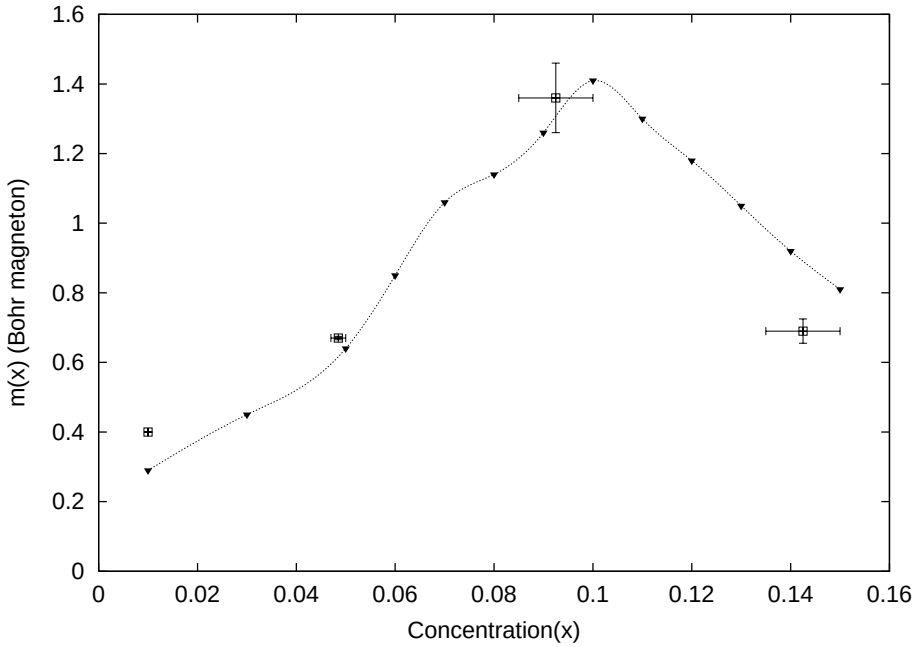

Fig. 1. Experimental values for Mn magnetic moment, with the error bars, in Bohr magnetons (open squares) and the results of the model (full triangles). The dotted curve is a guide for the eyes.

2 Experimental results

The samples were prepared by arc melting, starting from high purity elements Ni, B, C, Y and Mn, with $3N$ or better. Adequate amounts of the constituents were melted in a total mass of 5.5 g, in an arc-furnace with argon atmosphere and a Ti getter. We repeated five times the arc process to ensure the maximum homogeneity. Subsequently the ingots were annealed in vacuum at 1100 °C for five days, in quartz tubes protected by Ta foils. The samples were slowly cooled (134 °C/hour) to room temperature. The weight losses during the melting process were less than 1%. The room temperature X-ray powder diffraction analysis using the Fullprof software showed a single phase and a very small quantity ($\leq 5\%$) of a spurious phase in all compounds. The measured lattice parameters were obtained and the YNi_2B_2C lattice parameters were in quite good agreement with literature. The samples were prepared with Mn concentration x equal to 0.01, 0.05, 0.10 and 0.15.

The magnetic moment data, were extracted from isothermal magnetization measurements. These were performed using the SQUID technique (Magnetic Properties Measurement System - Quantum Design, model 2000), at 4.2 K with applied magnetic fields up to 5.0 T.

In order to determine the magnetic moments per Mn atom, an estimate of the impurity losses must be done. Due to the high vapor pressure of Mn the mass losses increase with nominal impurity concentration. To estimate the error bar in the Mn concentration we proceeded as follows: the higher limit of the horizontal bars is given by the nominal concentration, the lower one is given by corrected by the estimated Mn loss in the pseudo quaternary compound. This estimated loss was considered as given by the total observed loss in the compound minus the total loss in the pure one. The upper and lower limits in the Mn magnetic moment values were associated respectively to the lower and higher horizontal bar limits.

The obtained results for the magnetic moments, $m^{\exp}(x)$, as a function of nominal concentration x equal to 0.01, 0.05, 0.10 and 0.15, were 0.40, 0.67, 1.36 and 0.69 μ_B, respectively. These results are shown together with the error bars in Figure 1, where the experimental points are taken to be in the center of the error bars denoted as open squares. Note that for the 1% Mn concentration the above criterion is not applicable since the total mass loss of this compound was found to be less than in the pure compound.

3 The model

These quaternary body centered tetragonal compounds contain two sublattices: one is occupied by the Y atoms and the other by Ni and Mn atoms. The remaining atoms of this structure, namely boron and carbon, contribute in mediating a coupling Γ between the sublattices. Here we follow the same steps used in the cases of Laves phase systems [9] and of Heusler compounds [10], where we have adopted also a two sublattice model. The important difference with respect to the cases of [9] and [10] is that the density of states of the pure compound now is calculated from a first principles calculation. From this calculation, the moments of the density of $4d$ states can now be calculated. From these moments one can estimate the values of the parameters α_{nd} and ε^A defining the two sublattice model. Also we have numerically verified that the two sublattice model conserves the the moments of the density of

states associated up to the next nearest hopping in the lattice.

The electron propagator for the two sublattice systems, reads within the CPA approximation, in its simplest approach where charge transfer correction is replaced by parameter fit to experimental results. Within the two sublattice model one has:

$$G_k(z) = \begin{bmatrix} z - \varepsilon_k^{nd} & \Gamma \\ \Gamma & z - \Sigma(z) - \varepsilon_k^{3d} \end{bmatrix}^{-1} , \qquad (1)$$

where $z = \varepsilon + \mathrm{i}\delta$ and $n = 4$ or 5 corresponding to Y or rare earths sublattice respectively. Within the homothetic band picture approximation, one has:

$$\varepsilon_k^{nd} = \varepsilon^A + \alpha_{nd}\varepsilon_k^{3d} , \qquad (2)$$

where the energy ε^A fixes the position of the nd band with respect to the $3d$, α_{nd} accounts for its different width and Γ describes the intersublattice hoping. The CPA self energy for $3d$ electrons with spin σ defined by $\Sigma(z, \sigma; x)$ describes all the impurity induced disorder effects for concentration x and it is calculated using the values of the energy levels $\varepsilon_{\mathrm{Ni}}$ and $\varepsilon^{\mathrm{imp}}$. We take the inter sublattice matrix elements $\Gamma(x)$ as impurity concentration dependent (see later on) and independent of k and spin. In this way, within CPA, all impurity effects are included in the $3d$ band *via* the self energy. This approximation was tested in two different cases [9,10].

In order to describe the magnetic moments, a self consistent spin dependent impurity energy level must be introduced within the Hartree-Fock approximation:

$$\varepsilon_{i\sigma} = \varepsilon_i + U_i N_{i-\sigma} , \qquad (3)$$

where $N_{\mathrm{i},\sigma}$ is the ith atom occupation number and is Ni or Mn . The involved energy levels are: for a Ni atom $\varepsilon_i = \varepsilon_{\mathrm{Ni}}$, as obtained from the pure compound band structure calculation and for the Mn atom the energy level $\varepsilon_{\mathrm{Mn}} = \varepsilon^{\mathrm{imp}}$ is considered a parameter to be fixed later on.

The procedure to determine the self energy $\Sigma(z, \sigma; x)$ one starts from the CPA self-consistent equation:

$$\frac{(1-x)\left(\varepsilon_{\mathrm{Ni},\sigma} - \Sigma(z,\sigma;x)\right)}{1 - (\varepsilon_{\mathrm{Ni},\sigma} - \Sigma(z,\sigma;x)) g_{00,\sigma}^{3d3d}(z)} + \frac{x\left(\varepsilon_{\mathrm{Mn},\sigma} - \Sigma(z,\sigma;x)\right)}{1 - (\varepsilon_{\mathrm{Mn},\sigma} - \Sigma(z,\sigma;x)) g_{00,\sigma}^{3d3d}(z)} = 0, \qquad (4)$$

with the local Green's function:

$$g_{00,\sigma}^{3d3d} = \sum_k \frac{z - \varepsilon_k^{nd}}{(z - \varepsilon_k^{nd})(z - \Sigma(z,\sigma;x) - \varepsilon_k^{3d}) - \Gamma(x)^2} , \qquad (5)$$

where, for our case of Y compounds, $n = 4$ [11]. Clearly the $3d$ density of states can be modified *via* the hybridization $\Gamma(x)$. Its importance in understanding the x variation of the Mn magnetic moment will be shown later. In order to determine the Fermi level μ in terms of the occupation numbers $\mathrm{N_i} = \mathrm{N_{i\uparrow}} + \mathrm{N_{i\downarrow}}$ of the atoms i = Ni and Mn, one imposes the condition:

$$(1-x)\, N_{\mathrm{Ni}}^{(0)} + x N_{\mathrm{Mn}}^{(0)} = (1-x)\left[N_{\mathrm{Ni}\uparrow} + N_{\mathrm{Ni}\downarrow}\right] + x\left[N_{\mathrm{Mn}\uparrow} + N_{\mathrm{Mn}\downarrow}\right], \qquad (6)$$

where $\mathrm{N_i^{(0)}}$ are the number of $3d$ electrons of Ni obtained from the first principles calculation; N_{Mn}^0 was taken equal to $N_{\mathrm{Ni}}^{(0)} - \Delta Z$, the ΔZ is the charge difference, in this case 3 electrons. The $N_{i\sigma}$ is given by:

$$N_{i\sigma} = -\frac{1}{\pi}\int^{\mu} \mathrm{Im}\left[\frac{g_{00\sigma}^{3d3d}(z)}{1 - (\varepsilon_{i\sigma} - \Sigma)\, g_{00\sigma}^{3d3d}(z)}\right] . \qquad (7)$$

From equations (6) and (7) one extracts the Fermi level (μ), for a given self energy Σ and impurity energies $\varepsilon_{i\sigma}$. The solution of the coupled system of equations (3) to (7) furnishes the self consistent values for $N_{i\sigma}$ as a function of x and the concentration dependent local magnetic moment is given by $m_i(x) = \mathrm{N_{i\uparrow}}(x) - \mathrm{N_{i\downarrow}}(x)$.

4 Numerical results and conclusions

The numerical procedure starts with a first principles linear muffin-tin orbital(LMTO) calculation with the atomic sphere approximation(ASA) [12]. To the exchange-correlation energy was adopted the generalized gradient approximation (GGA) [14]. Since the borocarbide structure is rather open it was necessary to use two empty spheres [13]. We minimized the total energy assuming a fixed ratio of lattice parameters c/a equal to 2.9886 [15] and obtained lattice parameter a equal to 3.599 Å, in a good agreement with the experimental value $a = 3.526$ Å. The corresponding local density of states (DOS) for Ni$-3d$ and $\mathrm{Y} - 4d$ are shown in Figure 2, where the local DOS of $\mathrm{Y} - 4d$ was amplified.

From these band calculation results, we extracted, using the moments of the unperturbed $4d$ density of states, the values for the quantities $\varepsilon^A = 4.2\,\mathrm{eV}$ and $\alpha_{4d} = 2.9$. In view of our first principles band calculation, and by calculating the moments of the $4d$ density of states, the parameters of the two sublattice model could be estimated from the beginning.

It remains to specify the values for the parameters involved in the coupled equations (3–5). We use for the Coulomb interaction parameters the following values: $U_{\mathrm{Ni}} = 3.5\,\mathrm{eV}$ and $U_{\mathrm{Mn}} = 3.3\,\mathrm{eV}$, where as it must, U_{Mn} is smaller than U_{Ni}. We recall also that, in view of the calculated $3d$ bandwidth, these values are consistent with the adopted Hartree-Fock description of electron-electron interactions.

For the impurity energy we adopted positive values with respect to $\varepsilon_{\mathrm{Ni}}$, namely $\varepsilon^{\mathrm{imp}} > 0.$, since we consider only repulsive impurities (Co, Fe, Mn). Once the values of the Coulomb interaction, the impurity energy $\varepsilon^{\mathrm{imp}}$ and the values for the corresponding concentration x of the hybridization $\Gamma(x)$ were chosen and fixed, the coupled

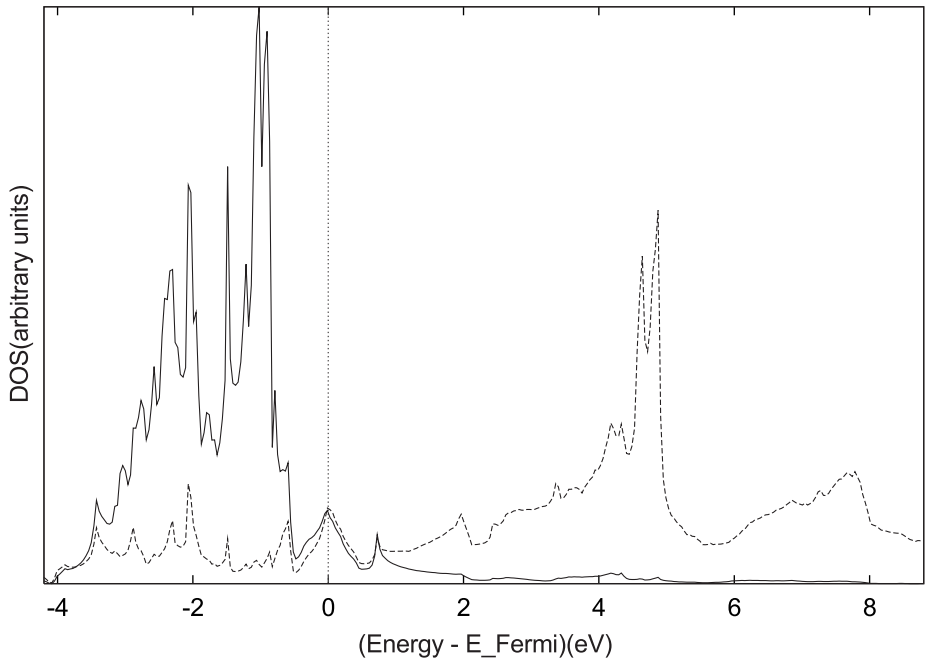

Fig. 2. Local density of states of $3d-$ Ni (solid line) and $4d-$ Y (dashed line) of the pure compound YNi_2B_2C.

system of equations (4–7) furnishes the values of the Mn magnetic moment, $m(x)$, for any value of the concentration. As a first comment, we have numerically verified that for $\Gamma(x)$ values in the range of 0.6 and 0.7 eV the impurity magnetic moment does not exists for impurity energy levels less than 1.0 eV. From this self-consistent numerical study one understands why experimentally observed Co and Fe impurities do not show any magnetic moment. This is due to the fact that a minimum repulsive strength for the impurity potential is necessary to magnetize the impurity.

Having adopted the above values for the Coulomb interactions, the parameter space is now restricted to $\varepsilon^{\rm imp}$ and to the strength of the intersublattice hopping values $\Gamma(x)$. The fitting to experiment was made using values of the intersublattice hopping $\Gamma(x)$ between 0.6 and 0.7 eV. Comparison to the experimental data suggests $\varepsilon^{\rm imp} = 1.62$ eV as the best value in order to reproduce the observed trend with x of the impurity magnetic moments, as shown in Figure 1 by small triangles. We have verified the importance of $\Gamma(x)$ hybridization to fit the experimental data. The calculated values of the magnetic moments on N_i and Y sites are very small and thus are not shown.

For increasing Mn concentration, the magnetic moment increases probably due to the piling up of the $3d$ states around the Fermi level due to the repulsive character of the impurity potential. Also the fitting indicates that $\Gamma(x)$ decreases with increasing x to arrive at a minimum value around $x = 0.10$. The decrease of $\Gamma(x)$ enhances more the piling up of $3d$ states since the effect of the extra hopping is to decrease the local density of states. Thus one has two *competing* contributions: the piling up of the $3d$ states by the repulsive d-electron scattering and the intersublattice hopping which tends to decrease the local density of states. We thus understand the decrease of $\Gamma(x)$ from 0.7 for $x = 0.01$ to attain the minimum value 0.6 for $x = 0.10$. Increasing the Mn concentration the piling up must be *compensated* by growth of the intersublattice hopping to 0.65 for $x = 0.15$. We conclude that the the maximum value of the Mn magnetic moment is associated to these two competing processes.

The two sublattice model introduced in [9] has been able to qualitatively account for the magnetic data in these materials, in particular the existence of a maximum of the magnetic moment for concentrations around 10%. We must stress that a *minimum* value for the impurity potential strength is necessary to induce the magnetic moment formation. Thus, one qualitatively understands why *only* Mn impurities do magnetize, since one needs a charge difference ($\Delta Z = 3$) to have a strong enough repulsive potential to produce piling up of states around the Fermi level.

Finally one must emphasize that the same electrons that superconduct are also responsible for moment formation, in contrast to the classical Abrikosov-Gorkov's picture. An application of the present picture to calculate the superconducting order parameter is now in progress.

This work was partially supported by the Brazilian Agencies: Conselho Nacional de Desenvolvimento Científico e Tecnológico (CNPq) and Fundação de Amparo a Pesquisa do Estado do Rio Grande do Sul (FAPERGS).

References

1. R.J. Cava, H. Takagi, H.W. Zandbergen, J.J. Krajewski, W. F. Peck Jr., T. Siegrist, B. Batlogg, R.B. van Dover, R.J. Felder, K. Mizuhashi, J.O. Lee, H. Elsaki, S. Uchida, Nature **367**, 252 (1994); R.J. Cava, H. Takagi, B. Batlogg, H.W. Zandbergen, J.J. Krajewski, W.F. Peck Jr., R.B. van Dover, R.J. Felder, T. Siegrist, K. Mizuhashi, J. O. Lee, H. Elsaki, S.A. Carter, U. Uchida, Nature **367**, 146 (1994).
2. L.F. Matheiss, T. Siegrist, R.J. Cava, Sol. State Commun. **91**, 587 (1994).
3. P. Ravindram, S. Sankaralingan, R. Asokamani, Phys. Rev. B **52**, 12921 (1995).
4. M. Divis *et al.*, Phys. Rev. B **62**, 6774 (2000).
5. C.C. Huellwarth, P. Klavins, R.N. Shelton, Phys. Rev. B **53**, 2579 (1996).
6. A.K. Gangopadhyay, A.J. Schuetz, J.S. Shilling, Physica C **246**, 317 (1995).
7. S.L. Bud'ko, M. Elamassalami, M.B. Fontes, J. Mondragon, W. Vanoni, B. Giordanengo, E.M. Baggio-Saitovitch, Physica C **243**, 183 (1995).
8. P. Soven, Phys. Rev. **156**, 809 (1967); A.J. Pindor, W.M. Temmerman, B.L. Gyorffy, J. Phys. F **13**, 1627 (1983); W.M. Temmerman, Z.S. Zetec, Comput. Phys. Rep. **5**, 173 (1987); J. Kudrnovsky, V. Drchal, Phys. Rev. B **41**, 7515 (1990); C.M. da Silva, A.A. Gomes, An. Acad. Bras. Ci. **68**, 139 (1996).
9. N.A. de Oliveira, A.A. Gomes, Mag. Magn. Mat. **114**, 283 (1992).
10. C.M. da Silva, D.E. Brandão, A.A. Gomes, J. Mag. Magn. Mat. **162**, 107 (1996).
11. C.M. da Silva, D.E. Brandão, A.A. Gomes, Physica C **162**, 107 (1998).
12. H.L. Skriver, *The LMTO Method* (Springer, New York, 1984).
13. R. Coehoorn, Physica C **228**, 331 (1994).
14. J.P. Perdew, S. Burke, M. Ernzerhof, Phys. Rev. Lett. **77**, 3865 (1996).
15. P. Ravindran, B. Johansson, C. Erikson, Phys. Rev. B **58**, 3381 (1998).